

# Organic & Biomolecular Chemistry

Accepted Manuscript



This is an *Accepted Manuscript*, which has been through the Royal Society of Chemistry peer review process and has been accepted for publication.

*Accepted Manuscripts* are published online shortly after acceptance, before technical editing, formatting and proof reading. Using this free service, authors can make their results available to the community, in citable form, before we publish the edited article. We will replace this *Accepted Manuscript* with the edited and formatted *Advance Article* as soon as it is available.

You can find more information about *Accepted Manuscripts* in the [Information for Authors](#).

Please note that technical editing may introduce minor changes to the text and/or graphics, which may alter content. The journal's standard [Terms & Conditions](#) and the [Ethical guidelines](#) still apply. In no event shall the Royal Society of Chemistry be held responsible for any errors or omissions in this *Accepted Manuscript* or any consequences arising from the use of any information it contains.

## COMMUNICATION

# Amyloid nanospheres from polyglutamine rich peptides: assemblage through an intermolecular salt bridge interaction\*\*

Cite this: DOI: 10.1039/x0xx00000x

DOI: 10.1039/x0xx00000x

www.rsc.org/

Rahul Mishra,<sup>a</sup> and Ashwani K. Thakur\*

**We show conversion of an amyloid fiber forming nucleation pathway of polyglutamine (polyGln) to a non-nucleated path, generating nanospherical amyloid particles. This is achieved by engineering an intermolecular salt bridge interaction between positively charged lysine and negatively charged glutamate residues, in two polyGln rich peptides. The mechanism of their formation is characterized by chromatography, infrared, fluorescence and imaging methods.**

Several soluble proteins and peptides get converted into insoluble, highly ordered fibrillar amyloids through self-assembly process.<sup>1</sup> Depending on the environment and the amino acid sequence, they generate fibres of varied strength and morphology.<sup>2,4</sup> Apart from the amyloid disease association, they serve as functional structures in catalytic scaffold,<sup>3</sup> bacterial coating,<sup>6</sup> and aerial hyphae.<sup>7</sup> By considering their fibrillar, biophysical and mechanical properties, they are fabricated into films,<sup>8</sup> nanowires,<sup>9</sup> liquid crystal phases,<sup>10</sup> and nanotubes.<sup>11</sup> Amyloid structure is stabilized by non-covalent interactions unlike the other engineered materials where strong covalent bonding forces are responsible for their strength.<sup>3</sup> It possesses characteristic cross- $\beta$ -sheet structure, about 10 nm diameter, micrometer length range and Young's modulus in gigapascal.<sup>12, 13</sup> Despite these facts, it remains largely unknown at atomic, molecular and interaction level about the formation of such structures, evolution of their morphological features and acquisition of exceptional properties. Although, a number of studies have been attempted on different amyloid systems to understand packing,<sup>14, 15</sup> physicochemical<sup>16</sup> and nanomechanical properties,<sup>17, 18</sup> new amyloid designs from a natural amyloid forming system by engineering non-covalent interactions are seldom explored.

In this context, one possible approach could be to choose a spontaneous homopolymeric aggregating amyloid system, in which a mutation in the background of similar sequence would show a

dramatic effect on its self-assembly to amyloid structure formation. Polyglutamine (polyGln) containing sequences represent one such system. Apart from their abundance in gliadins and gluten,<sup>19</sup> polyGln are present in human proteome with different lengths.<sup>20</sup> Aggregation of some of these sequences is involved in Huntington and other neurodegenerative diseases.<sup>21</sup> Recent, *in-vitro* studies on several polyGln peptides have shown that they aggregate in a nucleation polymerization pathway and generate beta sheet rich amyloid like fibers.<sup>22</sup> Moreover, the self-assembly of a four stranded beta sheet folding motif, in a 46 long polyGln peptide is inhibited by replacing glutamine to proline in the middle of the second beta strand (Table 1).<sup>23</sup> By using this model system, we have designed two polyGln peptides: one containing positively charged lysine (PepK) and the other having negatively charged glutamate (PepE) residues. We asked two explicit questions 1) what is the impact of charged amino acid substitution and 2) what is the influence of facilitating an intermolecular salt bridge interaction, on self-assembly and amyloid structure formation (Table 1).

Table 1. The name and sequence of peptides.

Name	Peptide sequence
PepQ*	K <sub>2</sub> [Q] <sub>9</sub> PG[Q] <sub>4</sub> Q[Q] <sub>4</sub> PG[Q] <sub>9</sub> PG[Q] <sub>9</sub> K <sub>2</sub>
PepP*	K <sub>2</sub> [Q] <sub>9</sub> PG[Q] <sub>4</sub> P[Q] <sub>4</sub> PG[Q] <sub>9</sub> PG[Q] <sub>9</sub> K <sub>2</sub>
PepE	K <sub>2</sub> [Q] <sub>9</sub> PG[Q] <sub>4</sub> E[Q] <sub>4</sub> PG[Q] <sub>9</sub> PG[Q] <sub>9</sub> K <sub>2</sub>
PepK	K <sub>2</sub> [Q] <sub>9</sub> PG[Q] <sub>4</sub> K[Q] <sub>4</sub> PG[Q] <sub>9</sub> PG[Q] <sub>9</sub> K <sub>2</sub>

\*These peptides are reported earlier to elucidate the beta sheet folding motif of PolyGln, during aggregation. A stretch of Q's (glutamine) represents a beta strand and PG (Pro-Gly) a turn position to make a four stranded beta sheet folding motif. The mutation of glutamine to proline, glutamate and lysine is done at 18 position in the second strand. Insertion of Pro at this position completely inhibits aggregation of PepP and thus critical in controlling folding and aggregation. N and C terminal lysines are added to enhance solubility of these peptides in aqueous buffer.<sup>23, 24</sup>

After disaggregation and solubilization, the purified PepK and PepE peptides were incubated for spontaneous aggregation at

37°C in PBS, pH 7.2<sup>25</sup> (supplementary method, M1). The aggregates generated at the end of reactions were imaged using transmission electron (TEM) and atomic force microscopy (AFM) (supplementary method, M2 & M3). TEM image analysis shows that PepK and PepE form elongated fibrous structures. PepK gives rise to tape like fibers (Fig. 1c and 1g) whereas PepE fibers (Fig. 1b and 1f) are wider and appear to be present in bundles (supplementary table 1).

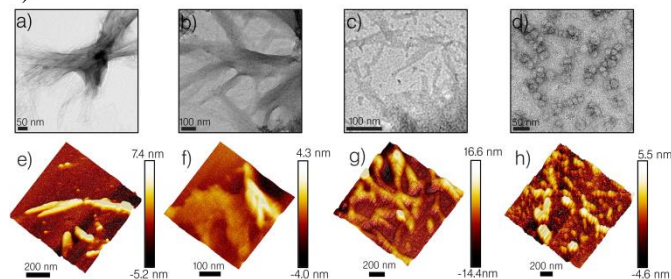


Fig. 1 Transmission electron microscopy images (a-d): a (PepQ), b (PepE), c (PepK), d (PepK+PepE). Atomic force microscopy height images (e-h): e (PepQ), f (PepE), g (PepK) and h (PepK+PepE).

Peptide fibrils match well in morphology and in dimensions with PepQ and earlier reported polyGln peptides.<sup>23, 26</sup> Excitingly, mixture of PepK and PepE yielded nanospherical, non-fibrous assemblies. They are observed in rings and linear chains (Fig. 1d and 1h). AFM imaging too shows similar structural features of peptide fibers and nanospheres (Fig. 1 e-h). In comparison to TEM, larger dimensions of fibers and nanospheres along with some morphological differences are observed by AFM analysis (supplementary table 1). These variations could be attributed to the differences in the nature of two techniques as well as the substrate used for sample adsorption.<sup>27-29</sup> On analyzing the microscopy results, approximately, a correction factor of 50% can be applied to AFM dimensions to report the similar dimensions of aggregates and nanospheres from TEM image analysis.<sup>29</sup> To confirm that nanospheres generated are specific to the mixture of PepK and PepE, combinations like PepQ+PepK, PepQ+PepE, PepP+PepK and PepP+PepE needs to be evaluated in future for aggregation and fiber/nanosphere formation. Interestingly, one combination (PepQ and PepE) tested yielded fibers and not nanospheres, suggesting that the other combinations may also form fibers (supplementary, Fig. S5).

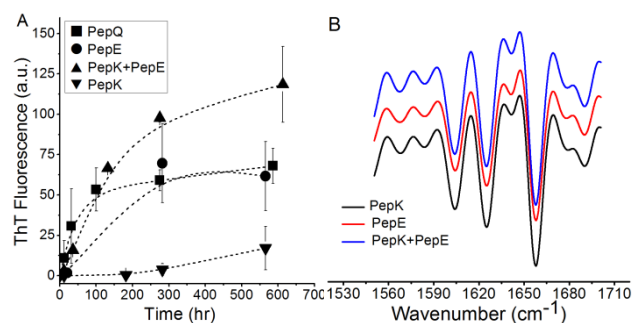


Fig. 2 A) ThT fluorescence of PepQ (■, 40 μM), PepE (●, 40 μM), PepK+PepE (▲, 40 μM each) and PepK (▼, 40 μM). Error bars represent standard error of mean calculated with minimum n = 2. B) FTIR spectra of mixture (PepK+PepE), PepE and PepK aggregates.

Fascinatingly, nanospheres by shape appear to be similar to oligomers present as intermediates in the amyloid fiber formation pathway of different amyloid forming polypeptides.<sup>30, 31</sup> Except some, oligomers bind weakly to amyloid staining dyes and show characteristic FTIR signature, quite different from the final fibers.<sup>32-36</sup> Strikingly, the nanospherical assemblies formed by PepK and PepE mixture show strong thioflavin T (ThT) binding comparable to fibers formed by PepK and PepE alone (Fig. 2A and supplementary Fig. S1). Additionally, they have polyGln fiber like FTIR signature bands at  $\sim 1605\text{ cm}^{-1}$ , Gln side chains;  $1625\text{--}1630\text{ cm}^{-1}$ ,  $\beta$ -sheet;  $1655\text{--}1660\text{ cm}^{-1}$ , C=O stretching of Gln<sup>37</sup> (Fig. 2B). Similar mature spherical amyloid particles were reported earlier from different proteins under heating,<sup>38</sup> pH change,<sup>39</sup> 6 M urea<sup>40</sup> and slow rotation<sup>41</sup> conditions.

In order to probe the mechanism of formation of nanospherical amyloids, we carried out spontaneous aggregation kinetics of PepK (40 μM) in PepE (40 μM) and individual peptides (40 μM), using RP-HPLC sedimentation assay. In this assay, an aliquot of an ongoing reaction is ultra-centrifuged and supernatant is injected in HPLC.<sup>25</sup> The area under the curve of a peptide peak obtained at 215 nm wavelength is converted to μM (micro molar) concentration using a standard curve developed for individual peptides of known concentration. The aggregation rates (μM/hr) (supplementary method, M4) prove that PepK aggregates sluggishly in comparison to PepE, which aggregates at almost half the rate as compared to PepQ (Fig. 3A). Remarkably, aggregation rate of the mixture (PepK in PepE) approached PepQ rate. In the mixture, the aggregation kinetics of PepK enhanced eight fold with respect to PepK alone, while that of PepE enhanced to a limited extent, both becoming very close to each other (supplementary, Fig. S2). Notably, in both cases, the nucleation phase (the lag time prior to aggregation) was reduced significantly (supplementary, Fig. S3). We hypothesize, that the sluggish aggregation behavior of PepK is due to positive charge of lysine at neutral pH, causing repulsion among monomers<sup>42</sup> and in the vicinity of glutamines resist the favorable interactions for stable nucleus formation and elongation to fibers.<sup>43</sup> But, due to comparable size of glutamate side chain to glutamine,<sup>44</sup> PepE showed aggregation efficiency closer to that of PepQ. The small difference found may be due to the negative charge on glutamate, slowing its elongation. In the mixture (PepK in PepE), the aggregation enhancement of PepK indicates the neutralization of lysine positive and glutamate negative charges by a salt bridge interaction, facilitating the formation of nanospherical assemblies.

Further, to investigate the mechanism of aggregation modulation in the mixture, a nucleation kinetic analysis of PepE in PepK and PepK in PepE was carried out (Fig. 3B). PolyGln peptides of different lengths aggregate in a nucleation dependent manner to form an aggregation prone, monomeric or multimeric critical nucleus, to initiate the elongation process of fiber formation.<sup>43, 45</sup> To observe the critical nucleus formation by PepE in PepK or vice versa, spontaneous aggregation of PepE at different concentrations, in PepK (40 μM) and PepK at different concentrations, in PepE (40 μM) was followed (supplementary method, M7). Initial twenty percent aggregation data from all the aggregation reactions was used

to generate a plot of monomer concentration (M) vs time<sup>2</sup> (sec<sup>2</sup>) [t<sup>2</sup> plot]. Then another plot between log of slopes obtained from t<sup>2</sup> plots vs log of starting monomer concentrations (M) [log-log plot] was generated. The slope obtained from the log-log plot contains an estimate of the critical nucleus size (n\*)<sup>25, 46</sup> (supplementary method, M7). It was seen that PepK and PepE peptides in their mixture, deviated from the nucleation pathway. The nucleation analysis data obtained did not fit in the log-log plot, necessary to establish the critical nucleus mediated nucleation pathway.<sup>43, 47</sup> On the other hand, PepE alone, tested for nucleation kinetic analysis fitted well to obtain a monomeric critical nucleus, as reported for polyGln sequence of similar length.<sup>45</sup> This clearly indicates that in the mixture (PepK in PepE), a non-nucleated mechanism is operating in place of nucleation polymerization path, leading to fast aggregation and the formation of nanospherical structures (Fig. 1d and 1h).

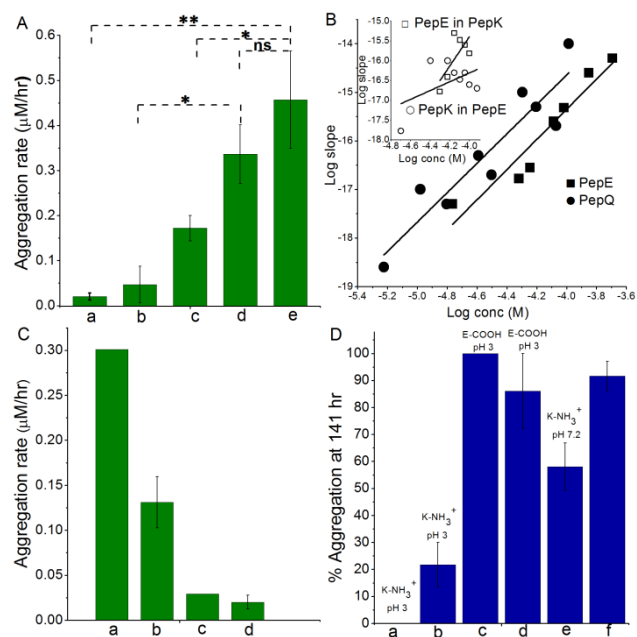


Fig. 3 A) Aggregation rates obtained from spontaneous aggregation kinetics of a (PepK; 40 μM), b (PepK; 80 μM), c (PepE; 40 μM), d (PepK+PepE; 40 μM each) and e (PepQ; 40 μM). Error bars represent standard error of mean for minimum n = 5 for 40 μM and n = 2 for 80 μM concentration. Statistical significance of measurement is represented by asterisks (\*\*, 0.001 < P < 0.01; \*, 0.01 < P < 0.05; ns = not significant, P > 0.05). B) Nucleation kinetics of PepQ (●, R<sup>2</sup> = 0.84), PepE (■, R<sup>2</sup> = 0.89), inset shows PepK in PepE (○, R<sup>2</sup> = 0.11) and PepE in PepK (□, R<sup>2</sup> = 0.39). C) Aggregation rates obtained from aggregation reaction: a (PepE; 40 μM with 4% w/w Pep E seeds), b (PepE; 40 μM without seeds), c (PepK; 40 μM with 4% w/w PepE seeds) and d (PepK; 40 μM without seeds). Error bars represent standard error of mean with minimum n = 6. D) % aggregation at 141 hrs at pH 3; a (PepK; 40 μM), b (PepK in PepE; 40 μM each), c (PepE; 40 μM), d (PepE in PepK; 40 μM each); e (PepK in PepE at pH 7.2; 40 μM each), f (Pep Q at pH 7.2 and pH 3.0; 40 μM). Error bars represent standard error of mean for minimum n = 2.

PepK alone was not tested for nucleation analysis as it was not aggregating within the concentration and time range of PepE, and even at high concentration of ~220 μM. The TEM and AFM analysis of this peptide, showing fibrous structures were carried after 23 days of incubation (Fig. 1c and 1g).

While the salt bridge between lysine and glutamate side chains of PepK and PepE looks evident, two possibilities for aggregation rate enhancement of PepK in PepE needs to be ruled out. The first is, in the mixture, a concentration of 40 μM PepE and 40 μM PepK peptides represent an effective concentration of 80 μM for polyGln. This concentration increase may enhance the rate of aggregation, as observed for different lengths of polyGln peptides (supplementary method M4).<sup>46, 48</sup> Interestingly, 80 μM reaction of PepK did not show significant aggregation and behaved similar to 40 μM PepK (Fig. 3A). The second possibility could be the seeding of PepK monomers by PepE aggregates in the mixture (PepK in PepE), as unlike PepK alone, PepE spontaneously aggregates at a faster rate. Remarkably, the aggregation rate of PepK did not increase on incubating with PepE seeds and it behaved like spontaneous aggregation kinetics (Fig. 3C). This result may be attributed to the buried glutamate side chain in PepE aggregates and, even if the glutamate side chains are exposed, PepE aggregates may associate with PepK monomers for the first round of elongation and not further as PepK itself is a constraint to elongation.

To strengthen the above results, we monitored spontaneous aggregation kinetics of these peptides at pH 3 (Fig. 3D). At this pH, since the glutamate side chain is neutral, PepE is expected to aggregate at a fast rate. Nonetheless, lysine will remain positively charged and PepK is expected to aggregate as in pH 7.2. Interestingly, PepE alone, displayed aggregation enhancement and became very close to PepQ. On the other hand, PepK did not show any aggregation and behaved as pH 7.2. When PepE and PepK were mixed in equimolar concentration at pH 3, PepK lost its aggregation tendency and behaved almost like pH 7.2. Similarly, PepE in this mixture aggregated at a fast rate like PepE alone at pH 3. Moreover, the kinetic behavior of PepE became almost equal to PepQ peptide at pH 7.2. PepQ aggregates in a similar fashion at pH 3.0 and pH 7.2 (Fig. 3D). This experiment authenticates that salt bridge is disrupted at pH 3.0 and glutamate side chain lost its interaction with lysine side chain. While in pH 7.2 it forms the salt bridge and influences the aggregation to a non-nucleated path, generating nanospherical amyloids.

In this communication, we showed that the introduction of lysine and glutamate residues at a specific position in a beta sheet folding motif of polyGln rich peptides, influence their aggregation behavior. But, both the peptides form amyloid fibers at the end of the reaction. By facilitating a salt bridge interaction between them, nanospherical amyloid structures were formed. These results were confirmed using TEM & AFM images, nucleation kinetic analysis, and pH dependent experiments. These nanospherical structures are obtained at the end of aggregation, bind ThT dye and shows polyGln fiber like FTIR signatures. The structure modulation obtained is mainly due to the change of nucleation pathway of normal polyGln to a non-nucleated path through salt bridge mediated interaction (supplementary, Fig. S4). This proof-of-concept can be considered as a starting point for manipulating polyGln sequences to generate multitude of amyloidic structures. This can be tested on other polyamino acid peptides having tendency to form amyloids.<sup>49</sup> It can be experimented by using a mutational approach in which permutation and combination of non-covalent interactions can be

applied to make and stabilize these structures. Such structures can be tested for exceptional properties to fit for bioengineering and nanotechnology applications. Moreover, they can act as tools to understand cellular toxicity of amyloid materials.<sup>3,50</sup>

## Notes and references

Department of Biological Sciences and Bioengineering, Indian Institute of Technology, Kanpur, Uttar Pradesh, India, 208016. E-mail: akthakur@iitk.ac.in

† Electronic supplementary information (ESI) available: Experimental details and calculations are given from M1toM8. Figures are represented from Fig. S1 to Fig. S5. See DOI:

AKT thanks Department of Biotechnology, Government of India (Grant No: BT/PR3041/NNT/545/2011) for financial support. R. Mishra thanks IIT Kanpur for providing PhD fellowship. We acknowledge All India Institute of Medical Sciences, New Delhi and Department of Chemical Engineering, IIT Kanpur for using TEM and AFM facilities.

- F. Chiti and C. M. Dobson, *Annu. Rev. Neurosc.*, 2006, 75, 333-366.
- B. Morel, L. Varela, A. I. Azuaga and F. Conejero-Lara, *Biophys. J.*, 2010, 99, 3801-3810.
- T. P. J. Knowles and M. J. Buehler, *Nat. Nano.*, 2011, 6, 469-479.
- Y. Hong, R. L. Legge, S. Zhang and P. Chen, *Biomacromolecules*, 2003, 4, 1433-1442.
- D. M. Fowler, A. V. Koulov, C. Alory-Jost, M. S. Marks, W. E. Balch and J. W. Kelly, *PLoS Biol.*, 2005, 4, e6.
- M. R. Chapman, L. S. Robinson, J. S. Pinkner, R. Roth, J. Heuser, M. Hammar, S. Normark and S. J. Hultgren, *Science*, 2002, 295, 851-855.
- D. Claessen, R. Rink, W. de Jong, J. Siebring, P. de Vreugd, F. G. H. Boersma, L. Dijkhuizen and H. A. B. Wösten, *Genes Dev.*, 2003, 17, 1714-1726.
- T. P. J. Knowles, T. W. Oppenheim, A. K. Buell, D. Y. Chirgadze and M. E. Welland, *Nat. Nano.*, 2010, 5, 204-207.
- T. Scheibel, R. Parthasarathy, G. Sawicki, X.-M. Lin, H. Jaeger and S. L. Lindquist, *Proc. Natl. Acad. Sci. U. S. A.*, 2003, 100, 4527-4532.
- A. M. Corrigan, C. Müller and M. R. H. Krebs, *J. Am. Chem. Soc.*, 2006, 128, 14740-14741.
- M. Reches and E. Gazit, *Science*, 2003, 300, 625-627.
- M. Sunde, L. C. Serpell, M. Bartlam, P. E. Fraser, M. B. Pepys and C. C. F. Blake, *J. Mol. Biol.*, 1997, 273, 729-739.
- A. W. P. Fitzpatrick, S. T. Park and A. H. Zewail, *Proc. Natl. Acad. Sci. U. S. A.*, 2013, 110, 10976-10981.
- A. D. Williams, S. Shivaprasad and R. Wetzel, *J. Mol. Biol.*, 2006, 357, 1283-1294.
- A. D. Williams, E. Portelius, I. Kheterpal, J.-t. Guo, K. D. Cook, Y. Xu and R. Wetzel, *J. Mol. Biol.*, 2004, 335, 833-842.
- F. Chiti, M. Calamai, N. Taddei, M. Stefani, G. Ramponi and C. M. Dobson, *Proc. Natl. Acad. Sci. U. S. A.*, 2002, 99, 16419-16426.
- R. Paparcone, M. A. Pires and M. J. Buehler, *Biochemistry*, 2010, 49, 8967-8977.
- H. Ndlovu, Alison E. Ashcroft, Sheena E. Radford and Sarah A. Harris, *Biophys. J.*, 2012, 102, 587-596.
- H. Wieser, *Food Microbiol.*, 2007, 24, 115-119.
- A. L. Robertson, M. A. Bate, S. G. Androulakis, S. P. Bottomley and A. M. Buckle, *Nucleic Acid Res.*, 2010, 39, D272-D276.
- H. T. Orr and H. Y. Zoghbi, *Annu. Rev. Neurosc.*, 2007, 30, 575-621.
- R. Wetzel, *J. Mol. Biol.*, 2012, 421, 466-490.
- A. K. Thakur and R. Wetzel, *Proc. Natl. Acad. Sci. U. S. A.*, 2002, 99, 17014-17019.
- C. A. Ross, M. A. Poirier, E. E. Wanker and M. Amzel, *Proc. Natl. Acad. Sci. U. S. A.*, 2003, 100, 1-3.
- B. O'Nuallain, A. K. Thakur, A. D. Williams, A. M. Bhattacharyya, S. Chen, G. Thiagarajan and R. Wetzel, in *Methods Enzymol.*, eds. K. Indu and W. Ronald, Academic Press, 2006, vol. Volume 413, pp. 34-74.
- S. Chen, V. Berthelie, J. B. Hamilton, B. O'Nuallai and R. Wetzel, *Biochemistry*, 2002, 41, 7391-7399.
- P. Mulvaney and M. Giersig, *J. Chem. Soc., Faraday Trans.*, 1996, 92, 3137-3143.
- B. Kokona, K. A. Johnson and R. Fairman, *Biochemistry*, 2014, 53, 6747-6753.
- L. A. Wade, I. R. Shapiro, Z. Ma, S. R. Quake and C. P. Collier, *Nano Lett.*, 2004, 4, 725-731.
- R. Kaye, Y. Sokolov, B. Edmonds, T. M. McIntire, S. C. Milton, J. E. Hall and C. G. Glabe, *J. Biol. Chem.*, 2004, 279, 46363-46366.
- J. Legleiter, E. Mitchell, G. P. Lotz, E. Sapp, C. Ng, M. DiFiglia, L. M. Thompson and P. J. Muchowski, *J. Biol. Chem.*, 2010, 285, 14777-14790.
- A. K. Thakur, M. Jayaraman, R. Mishra, M. Thakur, V. M. Chellgren, I.-J. L. Byeon, D. H. Anjum, R. Kodali, T. P. Creamer, J. F. Conway, A. M. Gronenborn and R. Wetzel, *Nat. Struct. Mol. Biol.*, 2009, 16, 380-389.
- E. Cerf, R. Sarroukh, S. Tamamizu-Kato, L. Breydo, S. Derclaye, Y. F. Dufrene, V. Narayanaswami, E. Goormaghtigh, J. M. Ruysschaert and V. Raussens, *Biochem. J.*, 2009, 421, 415-423.
- R. Carrotta, R. Bauer, R. Waninge and C. Rischel, *Protein Sci.*, 2001, 10, 1312-1318.
- J. W. Wu, L. Breydo, J. M. Isas, J. Lee, Y. G. Kuznetsov, R. Langen and C. Glabe, *J. Biol. Chem.*, 2010, 285, 6071-6079.
- J. Torrent, M. T. Alvarez-Martinez, F. Heitz, J.-P. Liautard, C. Balny and R. Lange, *Biochemistry*, 2003, 42, 1318-1325.
- K. Kar, C. L. Hoop, K. W. Drombosky, M. A. Baker, R. Kodali, I. Arduini, P. C. A. van der Wel, W. S. Horne and R. Wetzel, *J. Mol. Biol.*, 2013, 425, 1183-1197.
- H. Komatsu, N. Shinotani, Y. Kimori, J.-i. Tokuoka, K. Kaseda, H. Nakagawa and T. Kodama, *J. Biochem.*, 2006, 139, 989-996.
- M. R. H. Krebs, G. L. Devlin and A. M. Donald, *Biophys. J.*, 2009, 96, 5013-5019.
- I. Pallarés, C. Berenguer, F. X. Avilés, J. Vendrell and S. Ventura, *BMC Struct Biol.*, 2007, 7, 75-75.
- M. Hoshi, M. Sato, S. Matsumoto, A. Noguchi, K. Yasutake, N. Yoshida and K. Sato, *Proc. Natl. Acad. Sci. U. S. A.*, 2003, 100, 6370-6375.
- W. Wang and M. H. Hecht, *Proc. Natl. Acad. Sci. U. S. A.*, 2002, 99, 2760-2765.
- A. M. Bhattacharyya, A. K. Thakur and R. Wetzel, *Proc. Natl. Acad. Sci. U. S. A.*, 2005, 102, 15400-15405.
- T. E. Creighton, *Proteins: Structures and Molecular Properties*, Freeman, New York, 1983.
- K. Kar, M. Jayaraman, B. Sahoo, R. Kodali and R. Wetzel, *Nat. Struct. Mol. Biol.*, 2011, 18, 328-336.
- S. Chen, F. A. Ferrone and R. Wetzel, *Proc. Natl. Acad. Sci. U. S. A.*, 2002, 99, 11884-11889.
- F. Ferrone, in *Methods Enzymol.*, ed. W. Ronald, Academic Press, 1999, vol. Volume 309, pp. 256-274.
- N. Slepko, A. M. Bhattacharyya, G. R. Jackson, J. S. Steffan, J. L. Marsh, L. M. Thompson and R. Wetzel, *Proc. Natl. Acad. Sci. U. S. A.*, 2006, 103, 14367-14372.
- M. Fändrich and C. M. Dobson, *EMBO J.*, 2002, 21, 5682-5690.
- I. Cherny and E. Gazit, *Angew. Chem., Int. Ed.*, 2008, 47, 4062-4069.